Electronic Supplementary Material (ESI) for Dalton Transactions.

Supplementary Information

Rotation Configuration Control of the sp2 Bond in Diimidazole−dicarboxylate Linker for Isomerism of Porous Coordination Polymers

Qiubing Dong[a], Kai Ge[a], Minxing Zhang[b], Huijie Wang[a], Jingui Duan[a,*]

[a] State Key Laboratory of Materials-Oriented Chemical Engineering, College of Chemical Engineering, Nanjing Tech University, Nanjing 210009, China. Email: duanjingui@njtech.edu.cn.

[b] School of Chemistry and Chemical Engineering, Nantong University, Nantong, Jiangsu 226019, China

General Materials

All reagents and solvents were commercially available and used as received.

Synthesis of the ligand. Step 1: Dimethyl 3',5'-dibromo-[1,1'-biphenyl]-3,5-dicarboxylate (**a**) is purchased from the Macklin. The precursor **b** was synthesized through the classic Ullmann reaction. Mixing **a** (1.4 g, 1eq), 2-methylimidazole (1.4 g, 5eq), L-Proline (0.3 g, 0.8 eq), CuI (0.24 g, 0.4 eq), K_2CO_3 (1.35 g, 3eq) in the 100 mL double-neck flask, and adding 25 mL ultra-dry DMSO into the mixture under nitrogen atmosphere, heating to 125 ℃ for 48 h, after cooling to room temperature, the crude product was treated by the extraction with water and ethyl acetate. The organic phase with the product was purified by the silica gel column chromatography with the solvent of ethyl acetate/petroleum ether, the product **b** is the white powder. Step 2: Adding b (1.0 g, 1eq), NaOH (1.2 g, 10 eq) into the solution of THF/MeOH/H_2O (30/30/60 mL), and then heat to 80 ℃ overnight. After cool to room temperature, rotary evaporation of solvent, dropwise concentrated hydrochloric acid tile the solution to pH = 6, the product **L** precipitated. ^{1}H NMR (400 MHz, $CDCl_3$): 2.62 (s, 6H), 7.00 (d, 2H), 7.20 (d, 2H), 7.43 (s, 1H), 8.09 (s, 2H), 8.65 (s, 1H), 9.12(s, 2H), 12.74 (s, 2H).

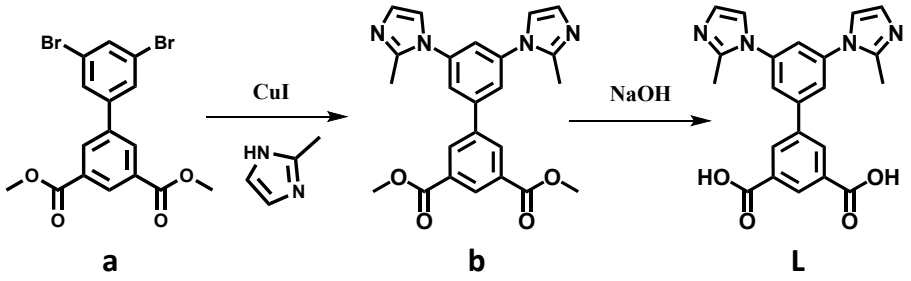

Figure S1. The procedure diagram for the synthesis of the ligand.

General Procedures

Thermogravimetric analyses (TGA) were performed using the STA 209 F1 (NETZSCH Instruments) thermo-microbalance, heating from room temperature to 600°C at a rate of 10°C min^{-1} under nitrogen flow.

Powder X-Ray diffraction (PXRD) patterns were tested with Bruker AXS D8 Advance (test conditions: 40 kV, 100 mA, CuKα, λ = 1.5418 Å, scanning range 5-30°). Simulated powder patterns from single-crystal X-ray diffraction data were generated using Mercury 1.4.2 software.

Gas adsorption isotherms were measured by soaking the as-synthesized samples in ultra-dry acetone for 3 days, and then the extract was replaced with fresh acetone 3 times every

day. Solvent-exchanged samples were then activated under dynamic high vacuum (<0.01 bar), held for 30 min at room temperature and then heated at 120 ℃ for 12h. In the adsorption measurements, the poly-grade gases (N_2, CH_4, CO_2, C_2H_6, C_2H_4, C_3H_6) were used. Gas adsorption isotherms were collected by using a volumetric adsorption instrument (Belsorp-mini from BEL Japan Inc.)

Ideal adsorbed solution theory (IAST)[4] was used to predict binary mixture adsorption as well as the separation factor from the experimentally obtained isotherms. In order to perform the integrations required by IAST, the single-component adsorption isotherms should be fitted by a proper model. There is no restriction on the choice of the model to fit the adsorption isotherm, but data over the pressure range under study should be fitted very precisely [5]. The dual-site Langmuir-Freundlich equation was used to fit the experimental data:

$$q = q_{m1} \cdot \frac{b_1 \cdot P^{1/n_1}}{1 + b_1 \cdot P^{1/n_1}} + q_{m2} \cdot \frac{b_2 \cdot P^{1/n_2}}{1 + b_2 \cdot P^{1/n_2}} \quad (1)$$

Here, P is the pressure of the bulk gas at equilibrium with the adsorbed phase (kPa), q is the adsorbed amount per mass of adsorbent (mol/kg), q_{m1} and q_{m2} are the saturation capacities of sites 1 and 2 (mol/kg), b_1 and b_2 are the affinity coefficients of sites **1** (1/kPa), and n_1 and n_2 represent the deviations from an ideal homogeneous surface.

Estimation of the isosteric heats of gas adsorption

A Virial-type_ENREF_41 expression comprising the temperature-independent parameters a_i and b_i was employed to calculate the enthalpies of adsorption for corresponding gas (at 273 and 298K) on NTU-69 and NTU-70. In each case, the data were fitted using the equation:

$$\ln P = \ln N + 1/T \sum_{i=0}^{m} a_i N^i + \sum_{i=0}^{n} b_i N^i \quad (2)$$

Here, P is the pressure expressed in Torr, N is the amount adsorbed in mmol/g, T is the temperature in K, a_i and b_i are virial coefficients, and m, n represent the number of coefficients required to adequately describe the isotherms (m and n were gradually increased until the contribution of extra added a and b coefficients was deemed to be statistically insignificant towards the overall fit, and the average value of the squared deviations from the experimental values was minimized).

$$Q_{st} = -R \sum_{i=0}^{m} a_i N^i \quad (3)$$

Here, Q_{st} is the coverage-dependent isosteric heat of adsorption and R is the universal gas constant.

Table S1. Crystal data and structure refinement of NTU-69 and NTU-70.

Name	NTU-70	NTU-69
Empirical formula	$C_{22}H_{16}CuN_4O_4$	$C_{66}H_{48}Cu_3N_{12}O_{12}$
Formula weight	463.94	1391.81
Space group	$P2_12_12_1$	$I2/a$
a / Å	11.3182 (4)	19.0772 (6)
b / Å	18.1653 (11)	32.4115 (10)
c / Å	19.1481 (9)	19.4415 (15)
α / °	90	90
β / °	90	β =100.577 (4)
γ / °	90	γ = 90
V / $Å^3$	3936.8 (3)	11816.8 (11)
Z	4	4
Dcalc /gcm^{-3}	0.783	0.782
μ /mm^{-1}	0.574	0.574
F(000)	948	2844
Θ rangeº	2.1 ， 25.1	1.9, 25.2
Index ranges	-13 ≤ h ≤ 11 -21≤ k ≤ 21 -22 ≤ l ≤ 21	-22 ≤ h ≤ 22 -36 ≤ k ≤ 38 -19 ≤ l ≤ 23
Tot., Uniq. Data	11190, 6147	40509, 10653
Flack	0.462	/
$R_{(int)}$	0.031	0.053
Observed Data [I > 2.0 sigma(I)]	5115	7046
R_1	0.0474	0.0602
wR_2	0.1264	0.2124
GOF	1.05	1.03

$R_1 = \Sigma||Fo| - |Fc||/|Fo|$; $wR_2 = [\Sigma w(\Sigma Fo^2 - Fc^2)^2/\Sigma w(Fo^2)^2]^{1/2}$

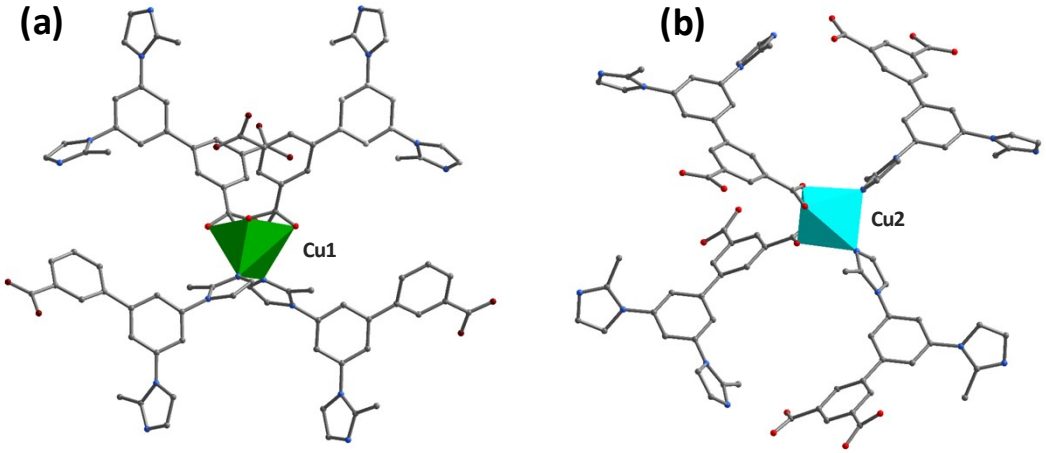

Figure S2 Two types of 4-c connected metal copper sites in NTU-69**.**

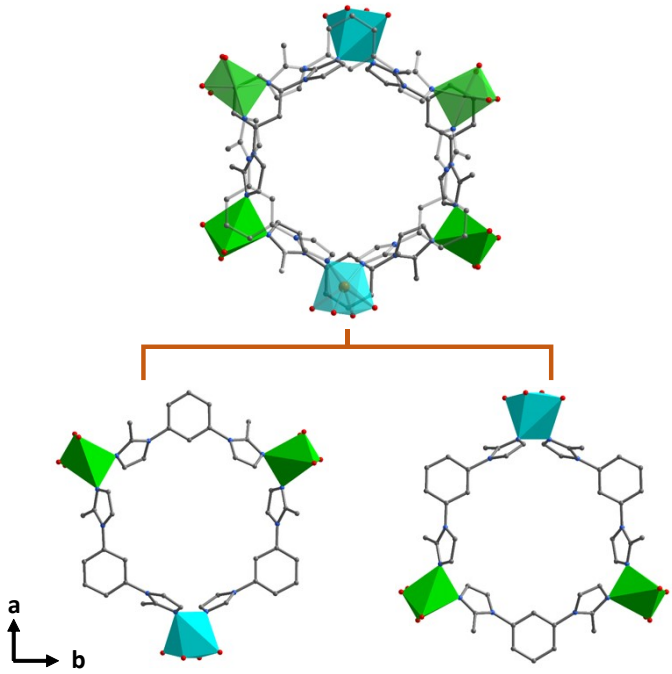

Figure S3. Pore packing view along c axis of NTU-69.

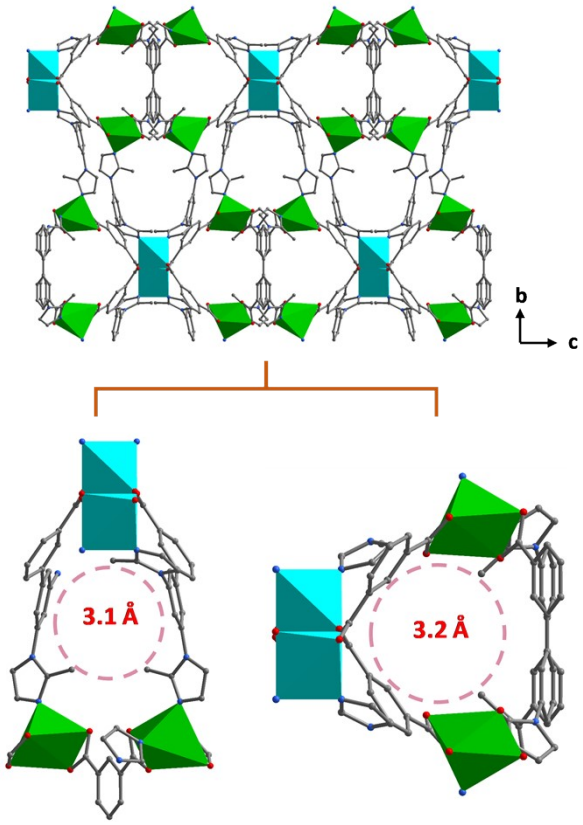

Figure S4. Packing view of NTU-69 along *a*-axis.

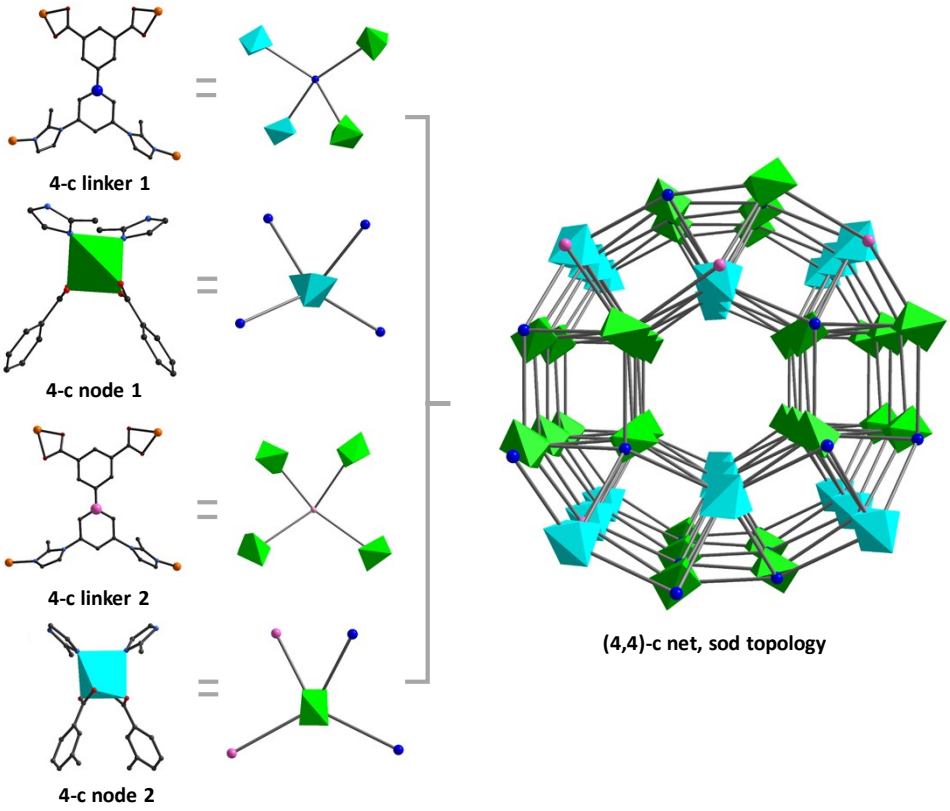

Figure S5. Topological analysis of NTU-69.

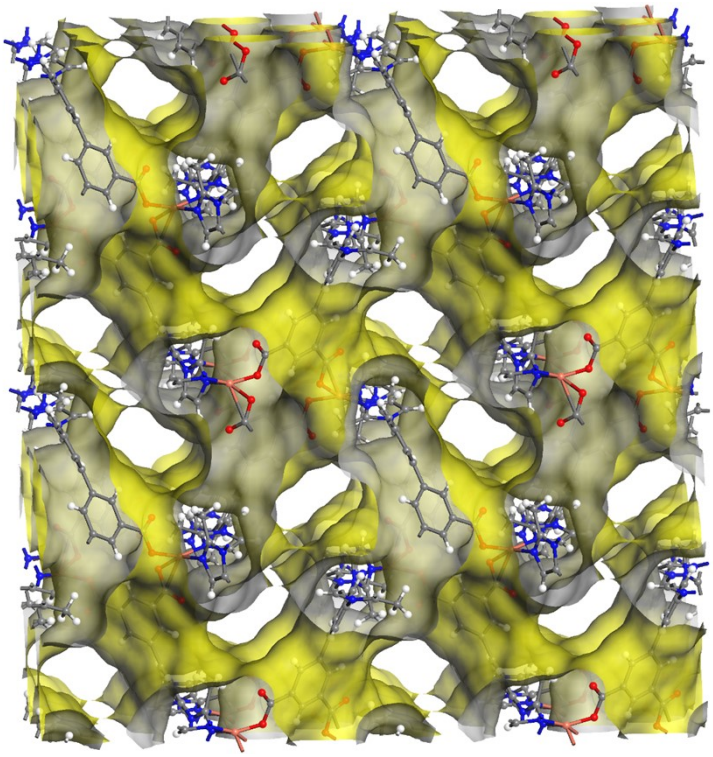

Figure S6. View of Connolly surface for NTU-69.

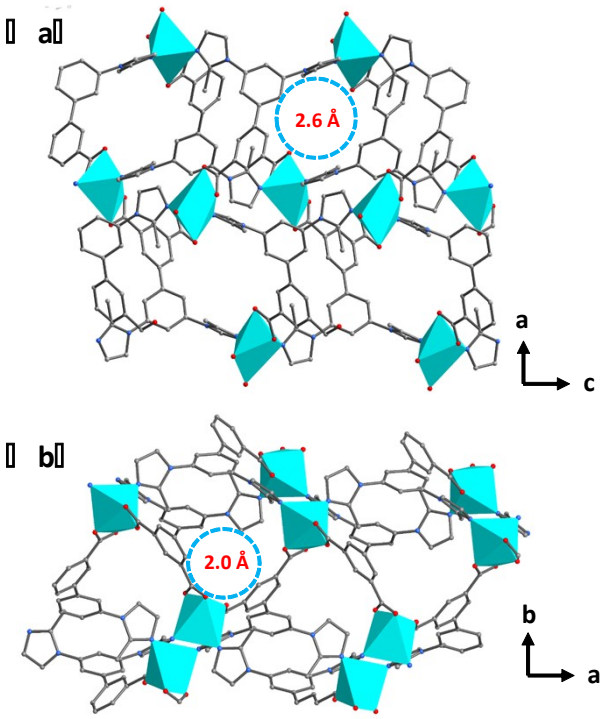

Figure S7. Pore view along *b*-axis (a) and *c*-axis (b) in NTU-70.

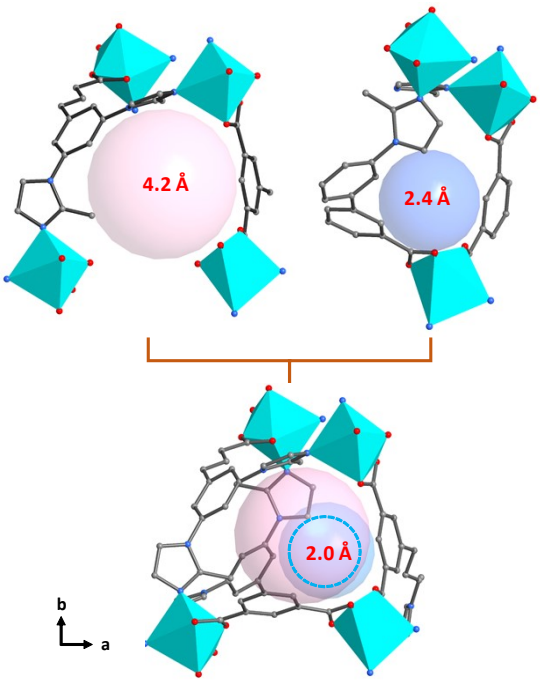

Figure S8. Pore view along c-axis in NTU-70.

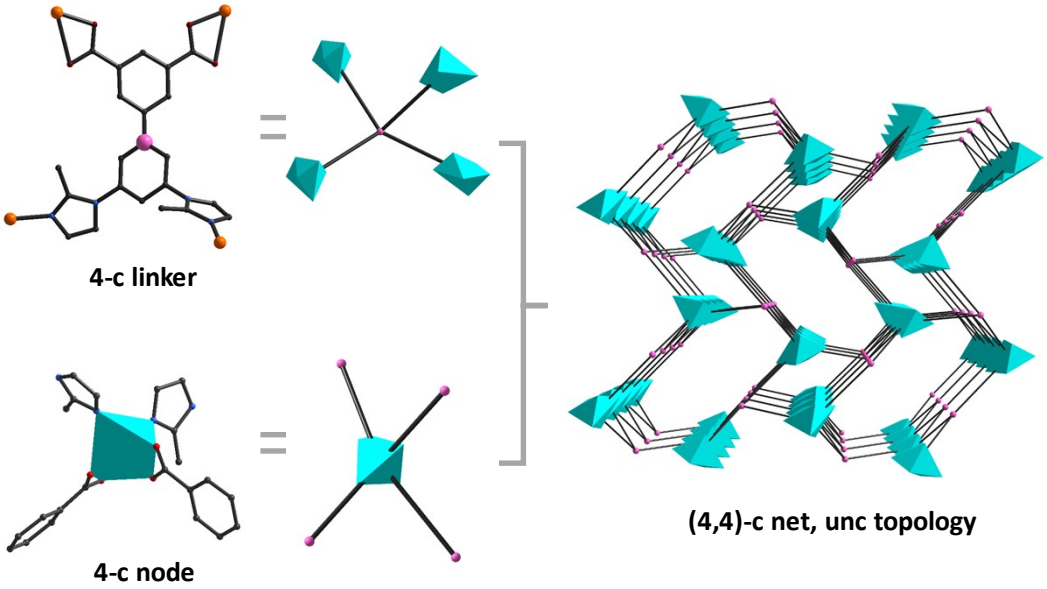

Figure S9. Topological analysis of NTU-70.

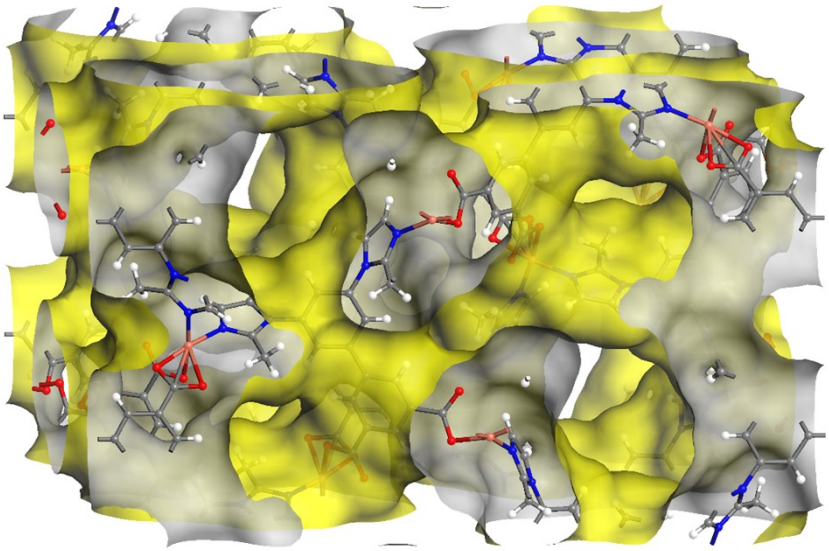

Figure S10. View of Connolly surface for NTU-70.

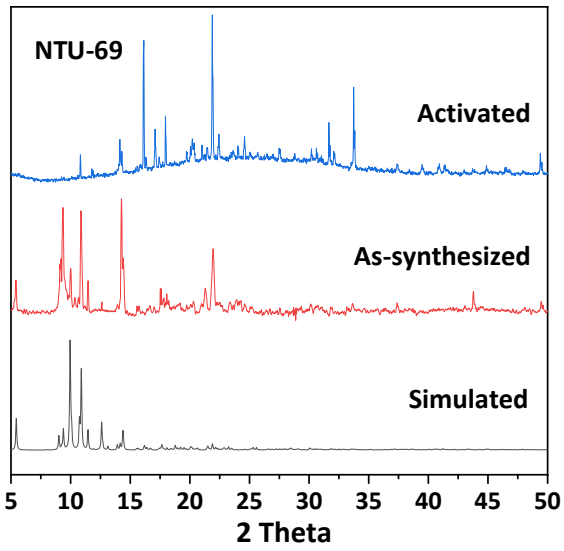

Figure S11. The PXRD patterns of NTU-69. The results indicate that the as-synthesized phase is pure, while the activated phase also changed some.

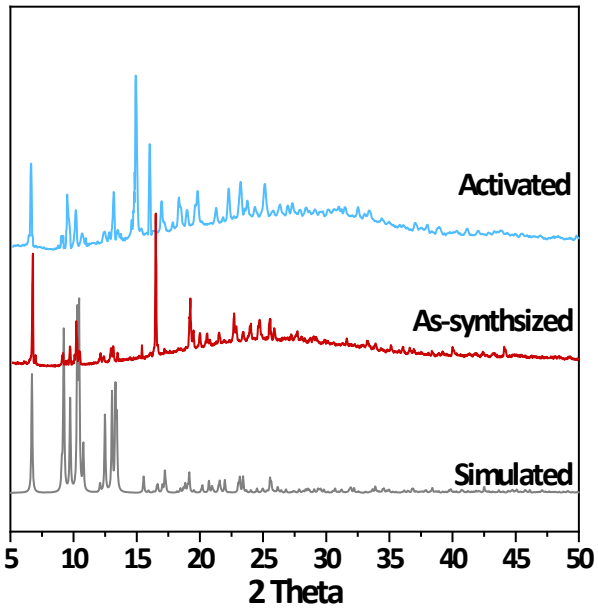

Figure S12. The PXRD patterns of NTU-70. The results indicate that the as-synthesized phase is pure, while the activated phase also changed some.

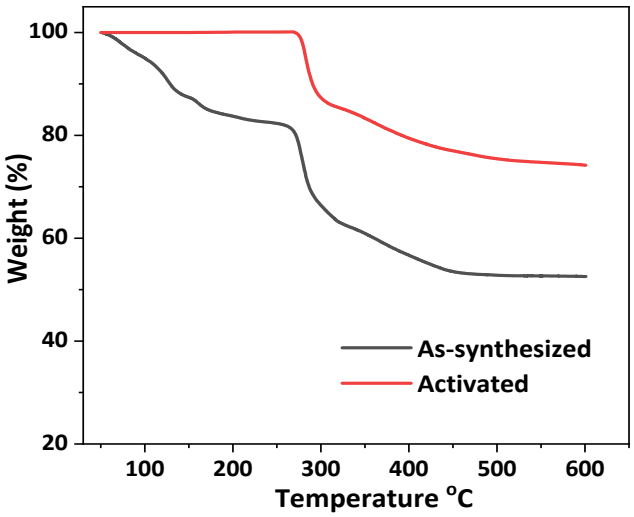

Figure S13. The thermogravimetric analysis results of NTU-69.

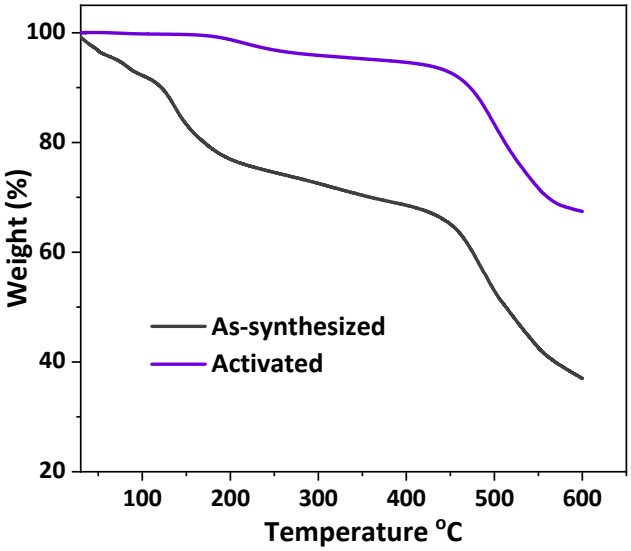

Figure S14. The thermogravimetric analysis results of NTU-70.

HBr / M/L	10 (μL)	15 (μL)	20 (μL)	30 (μL)
4 : 1	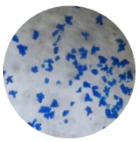	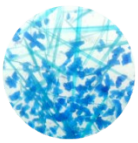		
8 : 1	\	\	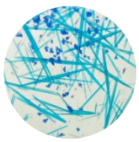	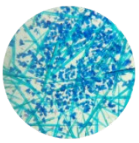
16 :1	\	\	\	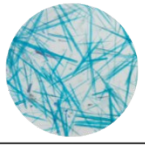

Figure S15. The pictures of corresponding products that synthesized according to the condition in Table 1.

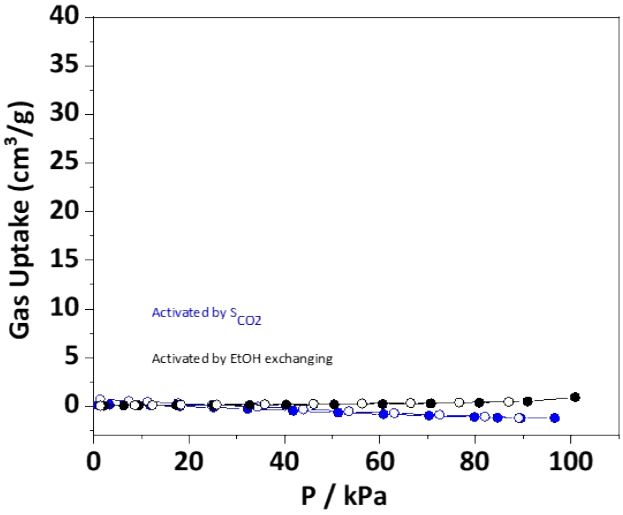

Figure S16. Negligible N_2 adsorption isotherms of NTU-69 at 77 K.

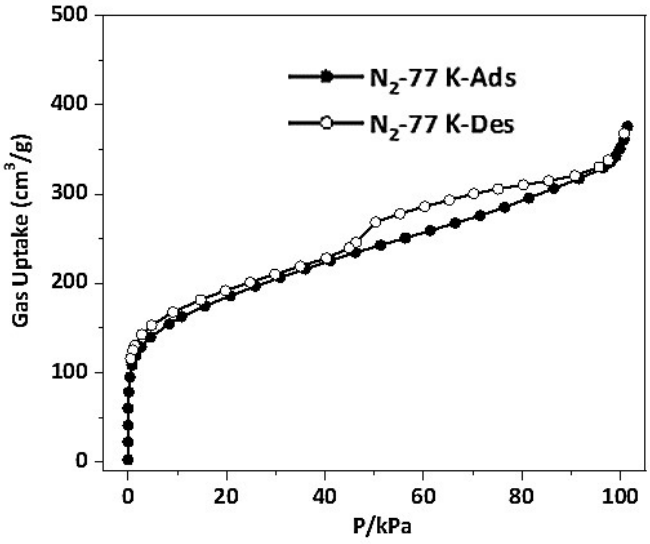

Figure S17. N_2 adsorption isotherm of NTU-70 at 77 K.

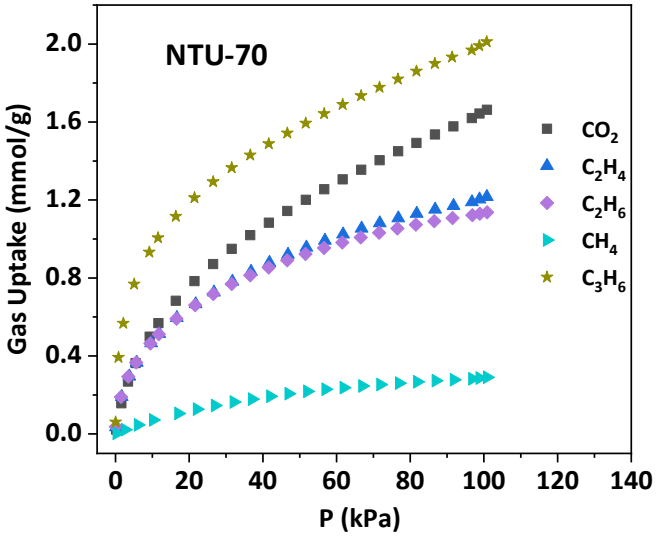

Figure S18. The adsorption isotherms of CO_2, C_2H_4, C_2H_6, CH_4 and C_3H_6 of NTU-70 at 273 K.

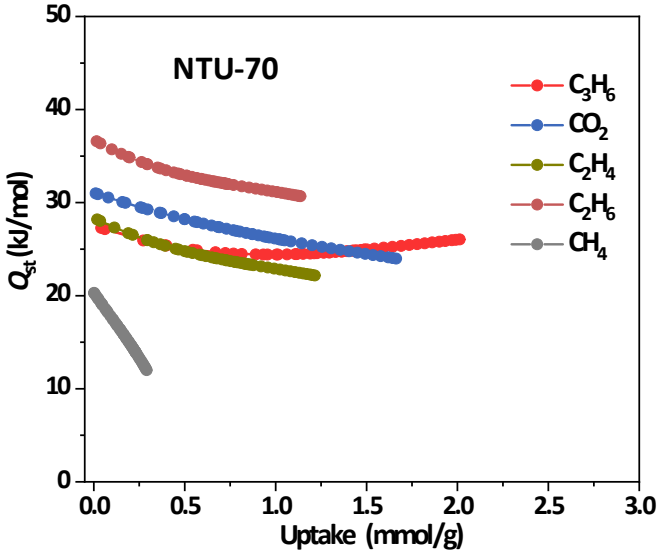

Figure S19. The adsorption isosteric heats of CO_2, C_2H_4, C_2H_6, CH_4 and C_3H_6 of NTU-70.